Analysis of winter dust activity off the coast of West Africa using a new 24-year over-water advanced very high resolution radiometer satellite dust climatology

Amato T. Evan,[1,2] Andrew K. Heidinger,[3] and Peter Knippertz[1,4]

[1]   A 24-year (1982–2005) winter daytime advanced very high resolution radiometer (AVHRR) data set has been processed utilizing a new over-water dust detection algorithm. The dust data are for the oceanic regions surrounding West Africa and provide a long-term remotely sensed continuous record of dustiness in the region. These AVHRR dust observations are comparable to dust records produced via the Total Ozone Mapping Spectrometer and Meteosat instruments. Strong positive correlations between the wintertime Jones North Atlantic Oscillation index and this dust record are observed across the entire oceanic region, corroborating earlier studies on the relationship between the two. Also consistent with previous investigations, we find more regional positive and negative correlations between dust and the wintertime Niño 3.4 index and summertime Sahelian precipitation, respectively. Also, unique to satellite studies of interannual dust variability over the North Atlantic, we develop a wintertime AVHRR normalized difference vegetation index time series for the Sahel region. A strong relationship is seen between tropical North Atlantic dustiness and this vegetation index, suggesting the possibility that vegetation changes in the Sahel play an important role in variability of downwind dustiness.

1.   Introduction

[2]   Soil derived aerosols are taking on an increased importance in scientific study as their roles in many different physical processes are coming to light. They make up a significant fraction of the total atmospheric aerosol signal and are the most prominent aerosol feature in visible satellite imagery [*Prospero and Lamb*, 2003]. The Sahara is the largest source of mineral aerosols [*Swap et al.*, 1996] and recent estimates put the amount of Saharan dust advected over the Atlantic at 230 tg annually [*Kaufman et al.*, 2003]. There is still a large degree of uncertainty associated with quantifying radiative forcing by mineral aerosols [*Sokolik et al.*, 2001] but there is evidence that the net effect is to displace the maximum heating from the surface to the dust layer [*Miller and Tegen*, 1998], with some estimates suggesting a net heating of the lower troposphere of ∼0.2 K per day when dust is present [*Alpert et al.*, 1998]. Additionally, dust plumes are thought to have an indirect effect on climate through the suppression of convection [*Prospero and Nees*, 1977; *Mahowald and Kiehl*, 2003] and through acting as cloud condensation nuclei [*Sassen et al.*, 2003]. A more technical aspect of the interest in dust advected over water is the resultant skewing of satellite sea surface temperature retrievals [*Nalli and Stowe*, 2002]. Saharan dust is also used to monitor the Saharan air layer's interactions with Atlantic tropical cyclones with satellite imagers [*Dunion and Velden*, 2004]. Several studies have suggested that iron from dust may be a controlling factor in phytoplankton growth [*Martin*, 1994; *Boyd et al.*, 2000], and dust deposition has been studied in relationship to Caribbean coral reef health [*Shinn et al.*, 2000], amphibian populations in Puerto Rico [*Stallard*, 2001], and the nutrient balance in the Amazon Basin [*Swap et al.*, 1992]. Furthermore, elevated dust concentrations may pose a significant respiratory health risk to people in the eastern USA and in other downwind locations [*Prospero*, 1999].

[3]   *Middleton and Goudie* [2001] and *Prospero et al.* [2002] have identified the Bodélé depression and western Mauritania as the major Saharan dust sources during the winter. *Brooks and Legrand* [2000] specify several areas in the Sahel region also important to winter dust mobilization. Source regions in the Sahara were thought to be fairly

---

[1]Department of Atmospheric Science, University of Wisconsin-Madison, Madison, Wisconsin, USA.
[2]Cooperative Institute for Meteorological Satellite Studies, University of Wisconsin-Madison, Madison, Wisconsin, USA.
[3]Office of Research and Applications, National Environmental Satellite, Data, and Information Service, NOAA, Madison, Wisconsin, USA.
[4]Now at Institute of Atmospheric Physics, University of Mainz, Mainz, Germany.

constant with regard to dust production because of the consistent lack of precipitation and vegetation found there. It had been proposed that the interannual variability in dustiness therefore is a result of changes in dust mobilization controlling parameters within the Sahel region, e.g., rainfall and vegetation cover [*Prospero et al.*, 2002; *Moulin and Chiapello*, 2004; *Chiapello et al.*, 2005]. However, recent work has shown that circulation changes can cause variability in dust aerosols associated with the Bodélé source region [*Washington and Todd*, 2005].

[4] The goals of this study are twofold: the first is to see to what extent we can reproduce observed relationships between dust and variables that are though to play an important role in interannual wintertime dust variability using a new and independent dust data set. These variables are the Niño 3.4, the Jones North Atlantic Oscillation (JNAO), and Sahel precipitation indices. In analyzing each variable we will discuss past work on the relationship between these variables and dustiness, as well as attempt to explain the possible mechanisms that could result in the observed relationships. The second aim of this paper is to introduce an AVHRR derived Sahelian normalized difference vegetation index (NDVI, for more information, see the NOAA GVI guide, http://www2.ncdc.noaa.gov/docs/gviug/) into the study of West African dust variability. This is done as an attempt to consider information about surface processes as they relate to observed dust aerosols. Previous to this study Sahelian NDVI has not been utilized in attempting to explain interannual West African dust variability.

[5] The remainder of the paper is organized as follows: In section 2 we discuss details related to the AVHRR dust data and compare the final dust product to other satellite records. In section 3 we present climatological findings related to the 24-year dust record. In section 4 we take these dust observations and look at the relationship between dustiness and the various climate indices listed above. These results are also compared to similar previous studies to find out to what extent we can corroborate their results. In section 5 we introduce and justify a Sahelian NDVI time series, and analyze the relationship between observed dustiness and this NDVI data. The paper concludes in section 6 with a summary and discussion of the findings.

2. Data Set

[6] The five channel AVHRR imager onboard the National Oceanographic and Atmospheric Administration (NOAA) series polar orbiting satellites provides daily global coverage at 4 km spatial resolution (at nadir) with a temporal range spanning 1982 to the present. Daily data for this analysis were collected for the region of 0°–40°N and 30°W–50°E for the months of JFM throughout the period of 1982–2005. A unique feature of this data set is that the AVHRR reflectance calibrations were taken from a new Office of Research and Applications (ORA) AVHRR reprocessing project. The results were obtained by translating the reflectance calibrations of the Moderate Resolution Imaging Spectrometer (MODIS) to AVHRR in a manner consistent with that of *Heidinger et al.* [2002]. Reflectance calibrations for pre-MODIS satellites were then determined by using a radiometrically stable desert target that had been characterized by MODIS.

[7] The algorithm used for dust detection [*Evan et al.*, 2006] was initially developed to improve the differentiation of optically thick dust plumes from cloud in NOAA's AVHRR operational cloud mask, the Clouds from AVHRR Extended System (CLAVR- x) [*McClain et al.*, 1985; *Heidinger et al.*, 2001; *Thomas and Heidinger*, 2004]. This algorithm relies on the depressed brightness temperature difference between the 11 and 12 μm channels exhibited by airborne dust [*Ackerman*, 1997; *Dunion and Velden*, 2004] as well as the increased spatial uniformity present under dusty conditions, which differentiates dust plumes from clouds [*McClain et al.*, 1985; *Jankowiak and Tanré*, 1992]. Full documentation of this algorithm as well as validation made by comparisons to the Aerosol Robotic Network station data is made by *Evan et al.* [2006].

[8] There are two main issues with the manner in which previous studies have utilized the AVHRR to study over-water airborne dust. The first is that these studies have equated the AOT in predominately dusty regions as being due to dust. However, this has lead to erroneous conclusions about the nature of dust over the North Atlantic, specifically dust seasonality, as the contribution to the AOT from smoke from biomass burning in Africa can skew the dust observations [*Swap et al.*, 1996; J. Prospero, personal communication, 2004]. The second issue is that the method for cloud clearing, differentiating cloudy from clear-sky or dusty pixels, as described by *McClain* [1989], which has been used in the AVHRR dust studies of *Swap et al.* [1996], *Husar et al.* [1997], and *Cakmur et al.* [2001], has been shown to be ineffective at differentiating optically thick dust plumes from cloud. Therefore there is likely little contribution to the dust statistics from more optically thick plumes in these previous studies [*Evan et al.*, 2006].

[9] Because this new algorithm flags a pixel as being dusty or not, we avoid problems of contamination of the dust statistics from smoke or other detected aerosols. The algorithm is capable of detecting dust plumes with an AOT of up to 4.5. However, a trade-off is that dusty pixels with an AOT less than 0.6 are not flagged as dust. This is done in order to minimize cloud and smoke contamination of the dust data. Although Saharan dust storms advected over water have been characterized as occurring in optically thick pulses rather than in a long continuous stream [*Carlson and Prospero*, 1972; *Jankowiak and Tanré*, 1992], we still need to further explore this assumption we are making, that Saharan dust variability can be quantified by analyzing only the optically thick dust plumes.

[10] To explore this assumption we made a simple test using the retrieved JFM AOT values for the 0.63 μm channel over the region of 15°–30°N and 10°–30°W, for the first 20 years of our data set. We chose this area because it is not near any sources of aerosols associated with biomass burning, and therefore the bulk of the AOT signal should be from dust aerosols. We calculated the fraction of AOT values within this region that were greater than 0.6, and compared that value to the annual average AOT over the same area. This enabled us to see if, on an interannual timescale, airborne dust with a retrieved AOT greater than 0.6 responds in a similar manner to the total retrieved AOT. Figure 1 is a graph showing how the annual changes of the fractional number of AOT values greater than 0.6 compares to annual changes of the total AOT. Visual inspection shows
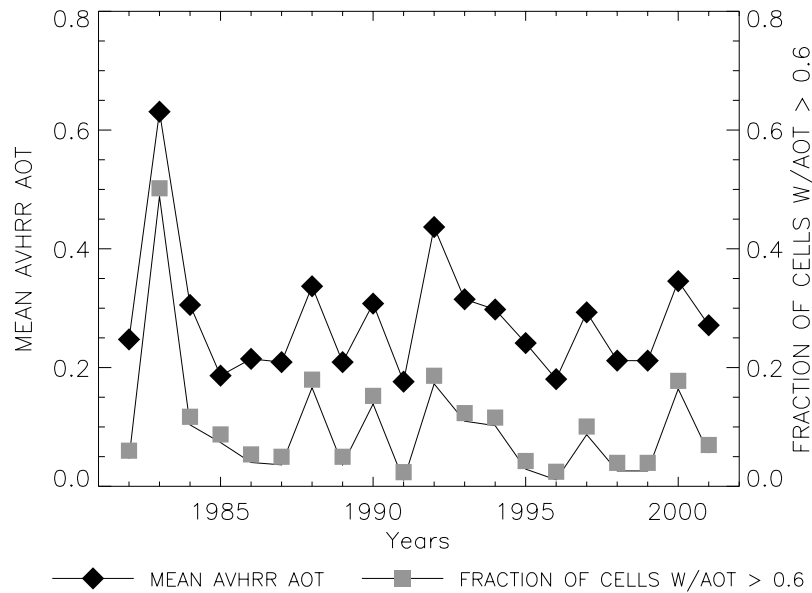
Figure 1. Comparison of JFM mean AOT at 0.63 μm to the fraction of cells with an AOT > 0.6 for 1982–2001 over the region of 15°–30°N and 10°–30°W. The shaded line and squares represent the fraction of cells with an AOT > 0.6 and is valued on the right-hand vertical axis. The solid line and diamonds represents the average AOT for the region and is valued on the left-hand vertical axis. The x axis represents years used for comparison. The two series have a correlation coefficient of 0.97, significant at the 99.9% level.

that the time series covary in a very similar manner, with the correlation coefficient between them being 0.97, significant at the 99.9% level (all significance values presented in the text are based on a two-tailed t score for the correlation coefficient). Therefore, at least to first order, we feel confident that although our dust algorithm is only responsive to more optically thick dust plumes, this is a reasonable way to characterize dust variability in the region.

[11] Another limitation of this dust detection method is that it does not provide any information about the total amount of dust present in any scene. This is an important point we wish to emphasize; the strength of this algorithm is that it is less affected by nondust aerosols and able to identify dust plumes with high AOT values. It does not provide absolute information about the amount of dust present nor does it provide information about plumes with an AOT less than 0.6. In theory one could get at an absolute dust amount by analyzing the AOT statistics in regions where they are confident that no other aerosols present will skew the results or by making comparisons with other instruments like the Meteosat or TOMS.

[12] The final dust statistic used in this paper is at half degree resolution (a fine enough resolution to resolve any large-scale dust features) and is the fraction of 4 km pixels that fall within a half degree grid cell that have been flagged as dusty. Consequently, a given half degree value for dustiness, for example 25%, can be thought of as corresponding to a grid cell that has, on average, 25% of its area containing an optically thick amount of dust, a grid cell that is completely obscured by dust 25% of the time, or some other combination of percent area and percent time statistics. However, the interpretation of total dust coverage as fraction of the time involved is closer to what the temporal and spatial data reflects. For each 55 × 55 km

grid cell, the daily dust fractions were averaged over each winter season (JFM) to create one 'seasonal' value per year per grid cell. If we had created monthly dust means and then averaged those to create an annual value for dustiness, we would be inadvertently weighing dust observations made during months that had some missing data. Therefore, by creating a single mean value per year from daily data, we average over the occasional missing orbit of data as well as two data gaps of roughly 20 days in the Five channel AVHRR daytime ascending satellite record which occur during February of 1985 and January of 1995.

[13] To demonstrate the effectiveness of this final dust product, in Figure 2 we have compared the AVHRR wintertime dust statistics to TOMS and Meteosat dust optical depth measurements over the region of 15°–30°N and 10°–30°W (TOMS and Meteosat data provided by I. Chiapello (unpublished data, 2005); see *Chiapello et al.* [2005] for details). The correlation between the three time series are all at least 0.87 and are all statistically significant at the 99.9% level. Considering that the AVHRR dust data set is a frequency statistic and not an AOT measurement, and that the AVHRR winter dust record consists of only JFM while the TOMS and Meteosat data includes December (which is generally a month of low dust activity), the high correlations are more evidence for the validity of the new AVHRR dust detection algorithm and the legitimacy of analysis of airborne dust via the frequency and spatial characteristics of the storms.

3. Climatology

[14] The dust data set was divided into three regions that exhibit spatially distinct interannual responses and regional dust maxima. Making these separations was useful in testing the extent of influence of potential large-scale
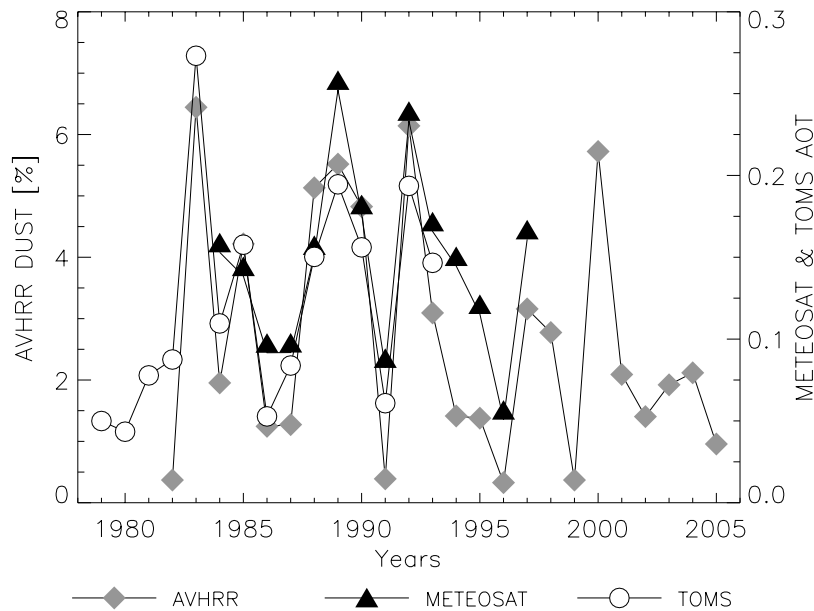
Figure 2. Comparison of plots of mean AVHRR JFM dust fraction to mean DJFM TOMS and Meteosat AOT. All values are averaged over 15°–30°N and 10°–30°W. Correlation between TOMS and Meteosat data is 0.92, AVHRR and TOMS is 0.92, and AVHRR and Meteosat is 0.87, all significant at the 99.9% level. Note that the values for the AVHRR dust signal do not represent the actual percent of area covered by dust but the area covered by very optically thick dust plumes. See section 2 for further details.

controlling factors of dust activity. Table 1 gives a description of these regions and their average dust fractions. Figure 3 shows where these regions lie on a map of the area under consideration. The ''subtropical Atlantic'' (STATL) region lies north of 15°N and is adjacent to the Sahara desert. As is seen in Figure 3 and Table 1, this is the region of minimal dust activity during the winter months, with the more southern latitudes containing higher mean dust fractions. This southern portion of the STATL area shows climatological means comparable to those of the other two regions considered. Some dust advected into this region may have an eastward return path toward the Iberian Peninsula [*Kaufman et al.*, 2003]. The ''tropical Atlantic'' (TATL) region lies between 0° and 15°N and extends east to 10°W. In Figure 3 the tongue of large mean values (roughly 5–15%) extending from the coast of Guinea to nearly 30°W is almost completely contained within the TATL region. This tongue is the most prominent feature in Figure 3 and is likely to represent the bulk of the dust that is advected toward the Americas during the winter months [*Swap et al.*, 1992]. Last is the ''Harmattan'' (HAR) region that covers the Gulf of Guinea. This region is so named as the dust detected in this area is ''Harmattan Haze'', dust entrained in the Harmattan, a northerly wind initiated by cold air out-

breaks from the midlatitudes that sweep down the western half of North Africa [*Goudie and Middleton*, 2001]. In the HAR region the area near the coastline has the highest climatological mean values. The gradient of mean values in the HAR region is steep, moving south from the coastline. This may result from washout of the dust particles by rainfall associated with the ITCZ, or low-level clear air being advected into the region as a result of the southerly monsoon wind. Additionally, the dust in this region was observed to exhibit a less depressed brightness temperature difference between the 11 and 12 μm channels, possibly indicative of a dust layer that is advected higher into the atmosphere [*Evan et al.*, 2006]. A more elevated dust layer is consistent with the deeper convective mixing at these more southerly latitudes. Furthermore, the lack of comparable average dust values to the west of the HAR region implies that dust over the Gulf of Guinea is not necessarily advected westward. The lack of high dust fraction values below about 5°N and west of the prime meridian may simply indicate the average position of the ITCZ during these winter months [*Hastenrath*, 1991].

[15] A plot of the dust time series for each region, as well as for the mean of all three regions (referred to as the TOTAL region), is displayed in Figure 4 along with a table

Table 1. Description of the Division of the Spatial Dust Signal[a]

	Latitude Range	Longitude Range	Mean Dust, % yr^{-1}	Number of Cells
Subtropical Atlantic (STATL)	15°–30°N	30°–10°W	2.68	815
Tropical Atlantic (TATL)	0°–15°N	30°–10°W	5.20	1026
Harmattan haze (HAR)	0°–10°N	10°W–10°E	6.73	408
Total dust (TOTAL)	0°–30°N	30°W–10°E	4.57	2249

[a]Included are the coordinates of the four regions, mean dust coverage values, and number of 0.5° grid cells contained within each area. All values only describe the over-water portions of the areas contained within the regions, which are then averaged over JFM. Note that the mean values do not correspond to the actual amount of dust covering an area (this number is higher), but they signify the fractional coverage of optically thick dust plumes as observed by the AVHRR dust detection algorithm.
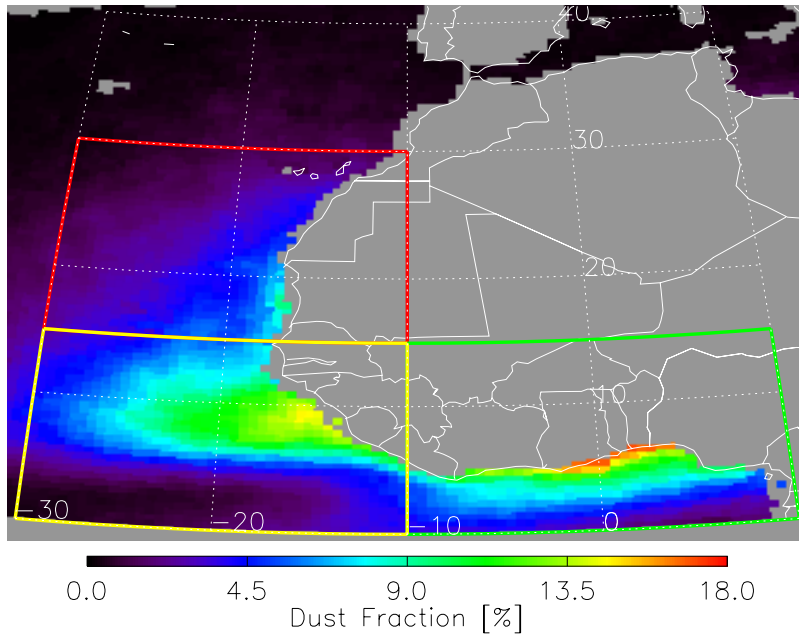
Figure 3. Image of the mean wintertime (JFM) grid cell dust fraction for 1982–2005. The boxes drawn over the various regions correspond to the areas where a single annual mean value was calculated. These regions will be referred to as the subtropical Atlantic (STATL, red box), tropical Atlantic (TATL, yellow box), Harmattan haze (HAR, green box), and total dust (TOTAL, all three boxes) regions. For further details, see Table 1. Note that the values for the mean AVHRR dust signal do not represent the actual percent of area covered by dust but the area covered by very optically thick dust plumes. See section 2 for further details.

of the correlation coefficients between the regions. The dust signals in all areas show variability, ranging from the maximums of 1983 to the near-zero values of 1996. Only the TATL region shows a statistically significant downward trend over the data set. The TATL and HAR regions are very highly correlated while the STATL time series appears to act more independently. This implies a large-scale control of the dust signal with some regional variability. This is possible,

as it has been shown that there are events that affect all three regions simultaneously [*Knippertz and Fink*, 2006].

4. Correlations

4.1. ENSO

[16] A relationship between Saharan dust activity during the winter, spring and fall seasons and ENSO was first
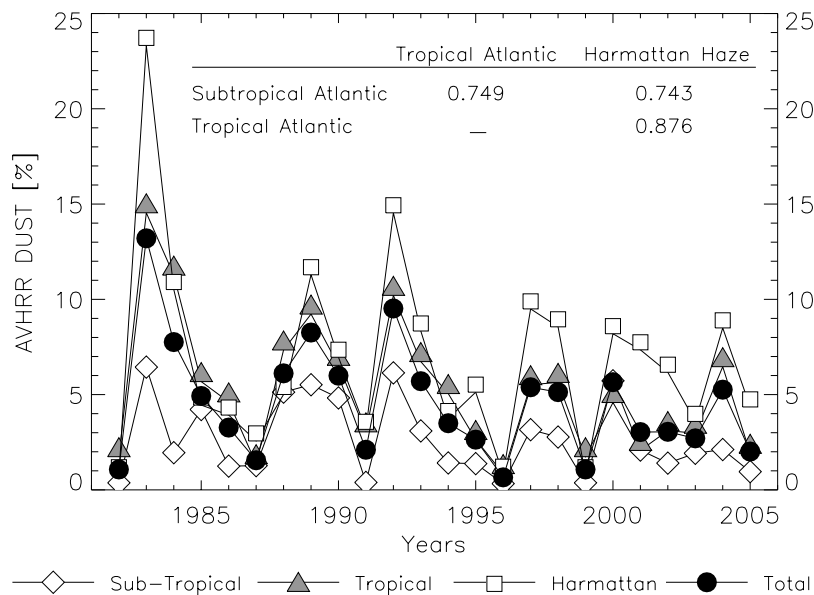

Figure 4. Plots of the time series for each dust region and correlation coefficients between the different regions. All correlations are significant at the 99.9% level.
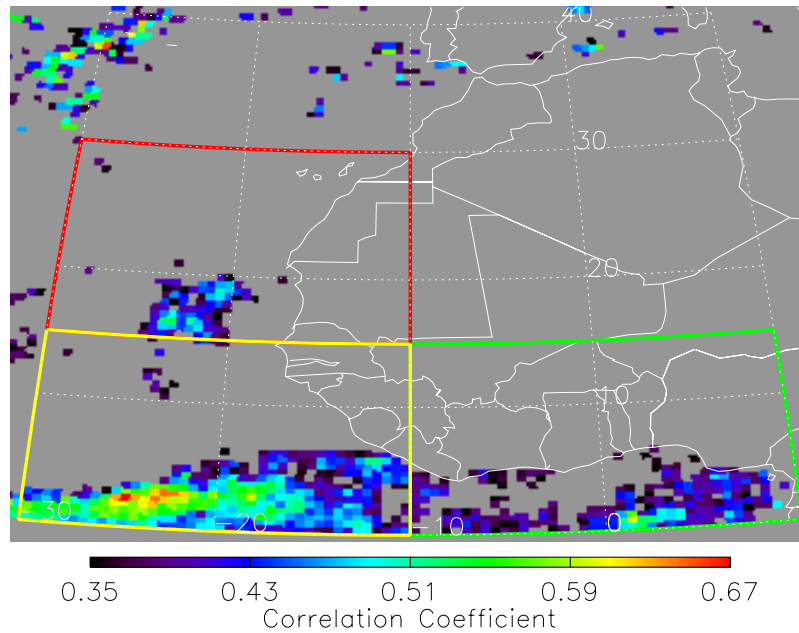
Figure 5. Correlation map of mean JFM dust fraction to mean DJFM Niño 3.4 index for 1982–2004. Regions of significant negative correlations were small and scattered, and therefore only positive correlations significant at the 90% level are shown. Description of boxed regions is the same as for Figure 3.

proposed using dust measurements taken in Barbados [*Prospero and Nees*, 1986]. They proposed that large-scale circulation changes related to ENSO could create anomalously strong trade winds over West Africa, bringing with them increased dust concentrations. *Prospero and Lamb* [2003] analyzed the Barbados data set of *Prospero and Nees* [1986] and found that most major dust events appeared to be associated with strong El Niño conditions during the previous year, possibly being indicative of a relationship between ENSO and rainfall in the Sahel region. However, this influence on rainfall is likely to be experienced only late in the rainy season [*Nicholson and Kim*, 1997]. *Mahowald et al.* [2003], using a combination of modeling results and station observations, did not find widespread correlations in and around West Africa between dust and the Niño 3.4 index.

[17] Figure 5 is a correlation map of the JFM AVHRR dust data set with the DJFM Niño 3.4 index (Niño 3.4 index data provided by the National Centers for Environmental Prediction (NCEP) reanalysis project at http://www.cdc.noaa.gov/ [see *Kalnay et al.*, 1996]). The inclusion of

December in the ENSO data reflects the fact that December is usually the peak month of the ENSO signal and better characterizes the general circulation related to ENSO during the wintertime (D. Vimont, personal communication, 2005). Figure 5 shows a large area of positive correlations spanning the Gulf of Guinea and stretching westward, which are mainly located in areas that have mean dust fractions of roughly 6.0% or less (Figure 3). A smaller area is found directly off the coast of Mauritania and Senegal, areas with climatological means of less than about 5.0% (Figure 3). Table 2 gives the correlation coefficients and the corresponding statistical significances for the different variables analyzed in this study, against all regions studied. From Table 2, only the HAR region shows strong correlations with the Niño 3.4 index that are statistically significant. The results of the correlations between the Niño 3.4 index and West African dust presented generally support the observational studies of *Prospero and Nees* [1986] and *Prospero and Lamb* [2003].

[18] ENSO is a persistent phenomenon with large-scale teleconnections. Because there may be a delayed response

Table 2. Correlation Coefficients Between the Dust Regions and Several Environmental Variables[a]

	Niño 3.4 Index: DJFM 1982–2005	Jones NAO Index: JFM 1982–2005	Sahel Rainfall Index: JJASO 1982–2003	Sahel NDVI: JFM 1982–2005
STATL	0.138	0.490[b]	−0.024	−0.359[c]
TATL	0.258	0.431[d]	−0.392[c]	−0.507[b]
HAR	0.373[c]	0.443[d]	−0.152	−0.325
TOTAL	0.281	0.478[b]	−0.257	−0.451[b]

[a]The temporal range considered for each correlation is also listed. All significance levels presented here and throughout the text are based on a two-tailed t score for the correlation coefficient.

[b]Correlation coefficient is statistically significant at the 97.5% level.

[c]Correlation coefficient is statistically significant at the 90% level.

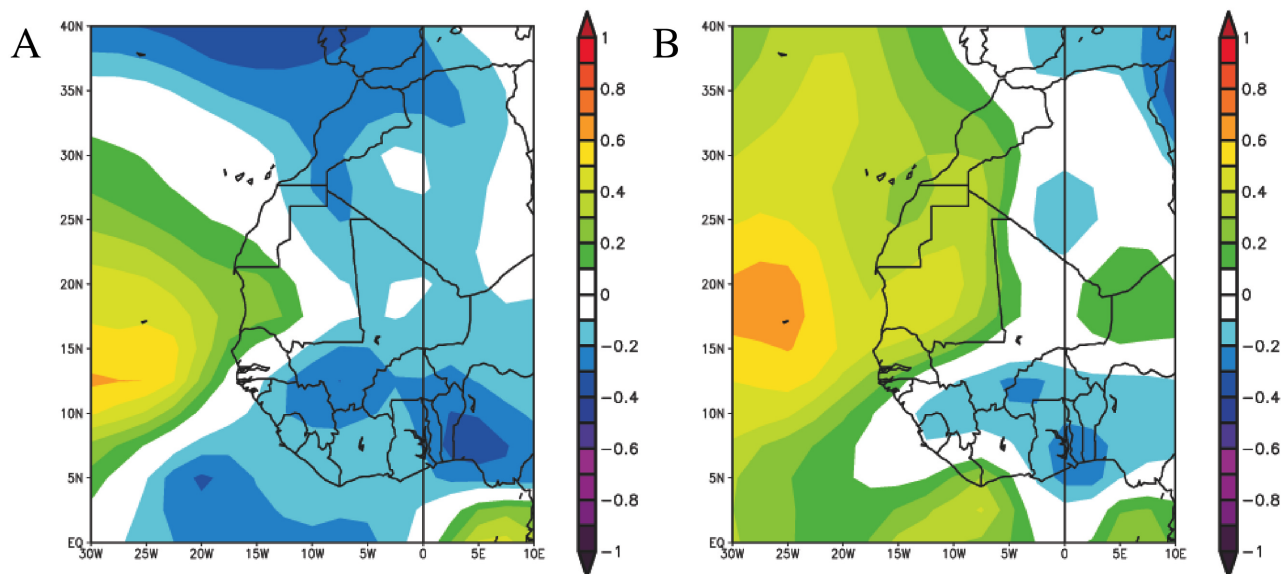[d]Correlation coefficient is statistically significant at the 95.0% level.

Figure 6. Correlation map of mean JFM (a) zonal and (b) meridional winds with the JFM Niño 3.4 index for 1982–2005. Image provided by the NOAA-CIRES Climate Diagnostics Center, Boulder, Colorado, from their Web site (http://www.cdc.noaa.gov/).

between ENSO and circulation shifts over West Africa and the North Atlantic, we explored correlations between the regional dust time series and the Niño 3.4 index, with the Niño index leading the dust time series from 3 months to a year. However, maximum correlations were found when comparing the DJFM Niño index to the JFM dust time series, as is done in this paper.

[19] Figure 6 is a correlation map of the mean JFM 925 mb zonal and meridional winds, and the Niño 3.4 index for 1982–2005. In Figure 6a, the zonal wind map, a region of negative correlations is present over the HAR and TATL regions, indicating that a positive ENSO event is associated with an enhancement of the Atlantic trades. This could indicate that more dusty air is being advected off West Africa at the more southerly latitudes, and would result in the observed correlations in the TATL and HAR regions in Figure 5. In Figure 6b, the meridional wind map, a similar widespread pattern of strong correlations across the TATL and HAR regions is not observed. Both Figures 6a and 6b show strong positive correlations in the STATL region. This is also near the same area that we observe increased correlation between dust and the Niño 3.4 index. This indicates that here a positive ENSO event is associated with reduction of the predominant trade flow. It is possible that dust advected into this area remains suspended for a longer amount of time than dust plumes to the north or south of this position.

[20] Although we have focused on explaining the relationship between dust and ENSO via circulation changes associated with ENSO, there may be other causal links between the two. One possibility is that the JFM ENSO signal is just reflecting summertime events, and that these summertime events are causing circulation changes which in turn affect processes that alter wintertime dustiness, like precipitation in the Sahel, which is discussed in section 4.3. However, this is purely speculation.

4.2. Jones NAO

[21] The NAO index is calculated by taking the difference between atmospheric pressures at stations near the NAO's southern center of action (the Azores high) and its northern center of action (the Icelandic low) [*Hurrell*, 1995; *Jones et al.*, 1997]. During a positive phase of the NAO there is a strengthening of the Azores high and a northward displacement of the northern midlatitude westerlies. *Moulin et al.* [1997] first proposed a control of dust storms in the Saharan and Sahel region by the NAO via analysis of summertime Meteosat data spanning 1983–1995 and annual Barbados dust data from 1964–1996. They suggested that a high positive phase of the NAO would bring drier conditions to North Africa, thereby increasing the opportunities for dust mobilization via decreases in soil moisture and dust washout. *Ginoux et al.* [2004], using the GOCART model, reproduced this correlation with wintertime dust and NAO data in a 15-year simulation with significant correlations found over the North Atlantic and Bodélé depression. *Mahowald et al.* [2003] found strong correlations between the NAO and West African dust source regions using a combination of modeling results and station observations. *Chiapello and Moulin* [2002] and *Chiapello et al.* [2005] found significant correlations over a large part of the North Atlantic when considering the wintertime data of TOMS and Meteosat with the former study also including the Barbados dust record. They proposed that a positive phase of the NAO would increase dust mobilization through the associated strengthening and repositioning of the trades over the Sahara.

[22] We initially tested the relationship between dust and the NAO by using the Hurrell NAO index, which is calculated by taking the difference between the normalized sea level atmospheric pressures between Lisbon, Portugal and Stykkisholmur, Iceland [*Hurrell*, 1995]. However, much more significant correlations were found across the
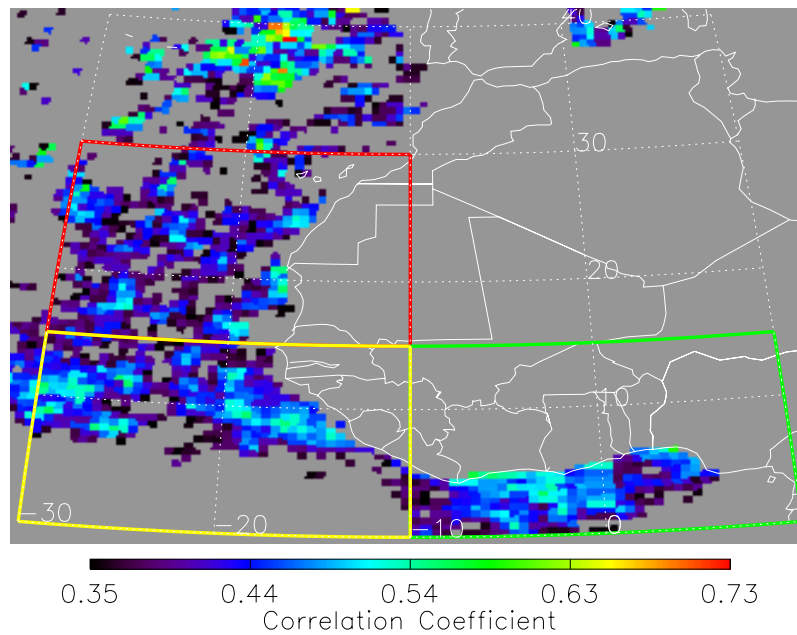
Figure 7. Correlation map of mean JFM dust fraction to mean JFM Jones NAO index for 1982–2004. Regions of significant negative correlations were small and scattered, and therefore only positive correlations significant at the 90% level are shown. Description of boxed regions is the same as for Figure 3.

entire area studied when correlations were made with the Jones NAO index (JNAO), the standardized pressure difference between southwest Iceland and Gibraltar [*Jones et al.*, 1997]. This is not surprising as the JNAO reflects a southern center of action that is closer to Africa. Mean monthly JNAO data were averaged over JFM for 1982–2004 and used as a winter index for correlation analysis (index data obtained through the Climate Research Unit, University of East Anglia, http://www.cru.uea.ac.uk/~timo/projpages/nao_update.htm).

[23] The correlation map of the JNAO and the dust signal is displayed in Figure 7. Strong correlations are found across the entire area being studied. The spatial patterns of Figure 7 are separated into three distinct areas: the HAR region, the STATL and TATL regions, and the oceanic area north of the STATL region. While correlations in the TATL and STATL areas are of a smaller magnitude than those in the other regions, they are the most widespread and cohesive. Table 2 shows that every region shows a strong and positive correlation with the wintertime JNAO index, the largest of which is found in the STATL region.

[24] As suggested by *Chiapello and Moulin* [2002] and *Chiapello et al.* [2005], it is possible that a strong Azores high close to West Africa will enhance the trade winds over the Sahara, thereby mobilizing dust. This trade enhancement could cause the spatial patterns in Figure 7 observed over the STATL and TATL regions. Additionally, the cluster of high correlations found off the coast of Morocco and near the Iberian Peninsula could be the result of dust advected off the continent and subsequently incorporated into the center of the Azores high, where it could remain suspended. This dust could also be part of the total flux off of West Africa that is caught up in the midlatitude westerlies and is advected over Europe [*Kaufman et al.*, 2003]. Also the

correlations over the Gulf of Guinea may be related to downstream processes that are initiated by a strong Azores high, such as a Harmattan surge [*Knippertz and Fink*, 2006].

[25] To further explore the patterns in Figure 7, we analyzed maps (Figure 8) of mean JFM meridional and zonal 925 mb winds as correlated with the Jones JFM NAO index for 1982–2001. Figure 8a is the zonal wind map. Here, strong negative correlations are observed across North Africa and into the subtropical North Atlantic, extending west from the central coastal region, and across the more southerly latitudes of West Africa and into the Gulf of Guinea. These large-scale spatial patterns indicate that in almost the entire area we use for our analysis of wintertime dustiness, the JNAO is associated with an enhancement of the zonal component of the trade flow. This enhancement could result in increased dustiness via increased dust mobilization over the source regions, or increased advection of already dusty air masses present over West Africa. This is generally consistent with the spatial patterns of Figure 7.

[26] Figure 8b is the meridional wind map. In general we see negative correlations over northern and southern West Africa, and positive ones over the more tropical oceanic areas (STATL and TATL regions). The implication is a strengthening of the northern flow across West Africa during positive NAO events, which is consistent with an increased Harmattan activity. Figure 8b also shows that dust advected off the continent over the TATL and STATL will be subjected to an increased southern flow. These meridional flows can explain the observed patterns in Figure 7, particularly the presence of strong correlations in the Gulf of Guinea, associated with the Harmattan, and the over the STATL and TATL regions, associated with dust plumes over the oceanic regions that are forced west along a more northward path. In Figure 8b, the region of positive corre-
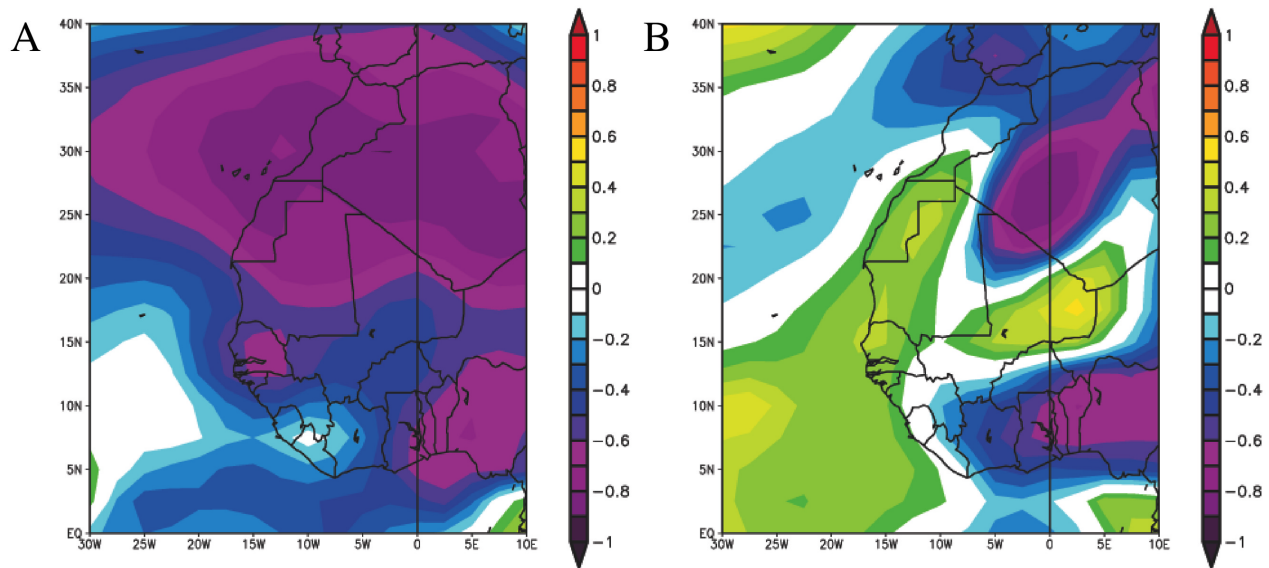
Figure 8. Correlation map of mean JFM JNAO index with mean JFM (a) zonal winds and (b) meridional winds. Image was provided by the NOAA-CIRES Climate Diagnostics Center, Boulder, Colorado, from their Web site (http://www.cdc.noaa.gov/).

lation over eastern Mali is over a region with very sparse observations and might not be very realistic.

[27] These widespread patterns in Figure 7, particularly those found in the STATL and TATL regions, and further to the north, generally corroborate the findings of *Moulin et al.* [1997], *Chiapello and Moulin* [2002], *Mahowald et al.* [2003], *Ginoux et al.* [2004], and *Chiapello et al.* [2005]. However, the coefficients of correlation that we observe are somewhat smaller in magnitude than those of the previous studies. This may simply be due to the time periods used in analysis, or small variability between this dust data set and those derived from other satellites.

4.3. Sahel Rainfall Index

[28] The Sahel region of Africa is the boundary between the Sahara desert and the tropical equatorial region of Africa, defined by mean annual rainfall amounts of 100–400 mm which is largely accumulated in the summer months [*Nicholson*, 1981]. The onset of a drought over the Sahel region in the late 1960s [*Nicholson*, 1981] has been studied in terms of a correlation with African dust using the Barbados dust data set [*Prospero and Nees*, 1977, 1986; *Prospero and Lamb*, 2003], the Meteosat infrared dust difference index (IDDI) over-land data set [*Brooks and Legrand*, 2000], with both summer and winter combined TOMS and Meteosat data [*Chiapello et al.*, 2005], and AVHRR aerosol optical thickness (AOT) data [*Swap et al.*, 1996], all finding, to varying degrees, a negative correlation between rainfall over the Sahel region and subsequent dust production.

[29] The Sahel rainfall index is based on the rotated principal component analysis of average June through September African rainfall presented by *Janowiak* [1988]. Stations within 8–20N, 20W–10E are obtained from the National Center for Atmospheric Research World Monthly Surface Station Climatology (from The Joint Institute for the study of the Atmosphere and Ocean, index data and

further information available at http://jisao.washington.edu/data_sets/sahel/). The mean JJASO Sahel rainfall index was used to determine if there is a relationship between rainfall in the Sahel during the previous year's rainy season and dust over the Atlantic during the wintertime.

[30] The correlation map in Figure 9 shows strong negative correlations contained within a region below 15°N, consistent with the observations of *Chiapello et al.* [2005]. These patterns are completely contained within the TATL region and are found to be partially over the tongue of large mean values extending over the Atlantic in Figure 3. Although this area is very localized, the magnitudes of these coefficients are relatively high. From Table 2 only the TATL region shows a relationship between observed dustiness and the rainfall index. These observations between precipitation and subsequent dustiness generally are in agreement with the results of *Prospero and Nees* [1977, 1986], *Swap et al.* [1996], *Brooks and Legrand* [2000], and *Prospero and Lamb* [2003], and *Ward* [1998] has shown that the summer climate of tropical Africa exhibits strong decadal variability that potentially exerts a strong influence on the correlation analysis presented here. In particular the Sahel rainfall has undergone long-term variations over the last century and shows a distinct upward trend between the dry early 1980s and the beginning of the 21st century. To explore this further we compared a detrended Sahel rainfall index to the TATL dust time series. Very weak and insignificant correlations were observed between the two, implying that the relationship between Sahel rainfall and dust are largely a result of the trends in the precipitation and dustiness over the span of the data set, and is not reflected on a year-to-year basis.

[31] It is possible that the previous year's JJASO Sahelian rainfall mediates dust mobilization by altering the soil moisture and/or creating soil situations less prone to mobilization, via aggregation or crusting [*Gillette*, 1999]. Alternatively, these correlations could be resulting from changes
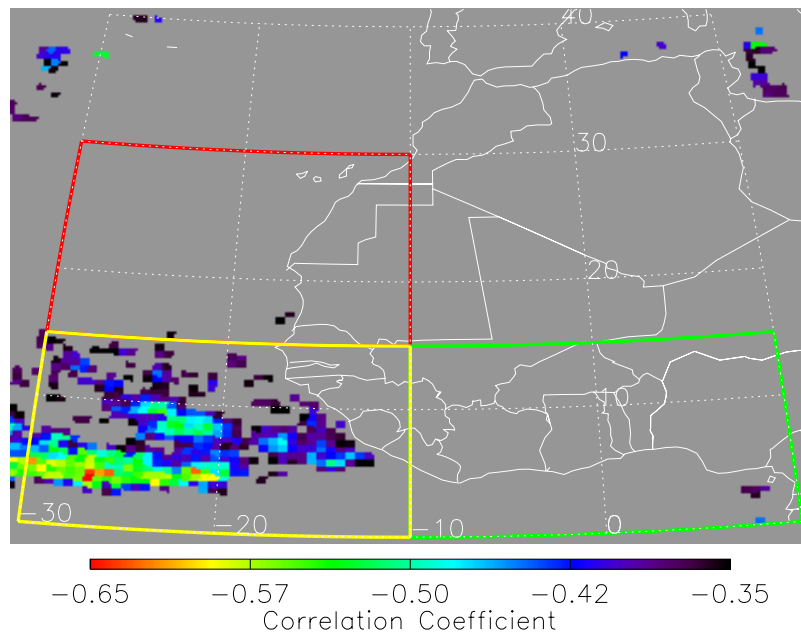
Figure 9. Correlation map of mean JFM dust fraction to mean JJASO Sahel rainfall index of the previous year for 1982–2003. Regions of significant positive correlations were small and scattered, and therefore only negative correlations significant at the 90% level are shown. Description of boxed regions is the same as for Figure 3.

in the atmospheric circulation that bring increased JJASO precipitation and subsequent JFM dustiness independent of each other. However, correlation maps of mean JFM zonal and meridional winds and the Sahel precipitation index did not show widespread patterns of strong correlations that support this theory. However, this does not necessarily discount it either as there are alternative ways to test this relationship that are beyond the scope of this paper. Another possibility is that the influence rainfall in the Sahel region exerts over wintertime dustiness is mediated through the response to the rainfall by vegetation. This possible three-way connection between rainfall, vegetation and dust is analyzed in the next section.

5. NDVI

[32] Only very recently have NDVI values in the Sahel been studied in relationship to regional dustiness. *Zender and Kwon* [2005] compared NDVI over the eastern Sahel, among other areas, to dustiness in the same region as seen by the TOMS. They found a lagged correlation between NDVI and dustiness, where peak dustiness occurred 9–10 months after the initial greening of the Sahel due to the summertime precipitation. However, this study analyzes the seasonality of NDVI and dust over the eastern Sahel and gives no indication if interannual variability in greenness of the Sahel is related to dust variability. In models, vegetation cover has been found to exert strong controls on dust emission [*Gillette*, 1999; *Engelstaedter et al.*, 2003]. However, in general, there is a lack of long-term observational satellite studies that have been made in order to investigate the findings of the modeling community. These types of studies are difficult as observations of NDVI in more barren areas are difficult due to the type of vegetation present

[*Zender and Kwon*, 2005] and because the retrieved NDVI values may be affected by atmospheric dust loadings.

[33] To address these difficulties we compared NDVI values across the Sahel with the Sahel precipitation index from the previous section. We expect that vegetation in the Sahel should be well correlated with the precipitation from the previous JJASO, and that a strong covariance between the two should, at least to first order, show that NDVI in the Sahel is responding to vegetation changes. The correlation map of mean JFM NDVI and the JJASO Sahel rainfall index in Figure 10 shows very strong, positive correlations across the entire Sahel region and further to the south. Positive feedbacks between vegetation and Sahel precipitation have been observed, particularly with regards to regime shifts in the Sahel [*Foley et al.*, 2003]. In light of these findings it is not surprising that we find such strong correlations between the Sahel NDVI and precipitation.

[34] To create a JFM NDVI time series reflective of Sahelian vegetation that can be used for comparison with the larger dust signal, an annual mean NDVI value was calculated for the region of $10°–20°N$ and $20°W–10°E$, shown as the red boxed area in Figure 10. The boundaries of this region were chosen in order to be consistent with the position of the rainfall stations used in creating the Sahel rainfall index. While the northern and southern boundaries may exceed the defined Sahel area, variability in these areas is likely very small, if not nonexistent, and therefore no efforts were made to exclude these regions from the NDVI time series. The correlation coefficient between the JFM Sahel NDVI time series and JJASO Sahel rainfall index is 0.626, significant at the 99.8% level. Widespread significant correlations were still seen when correlating the detrended Sahel precipitation and NDVI time series, implying the two
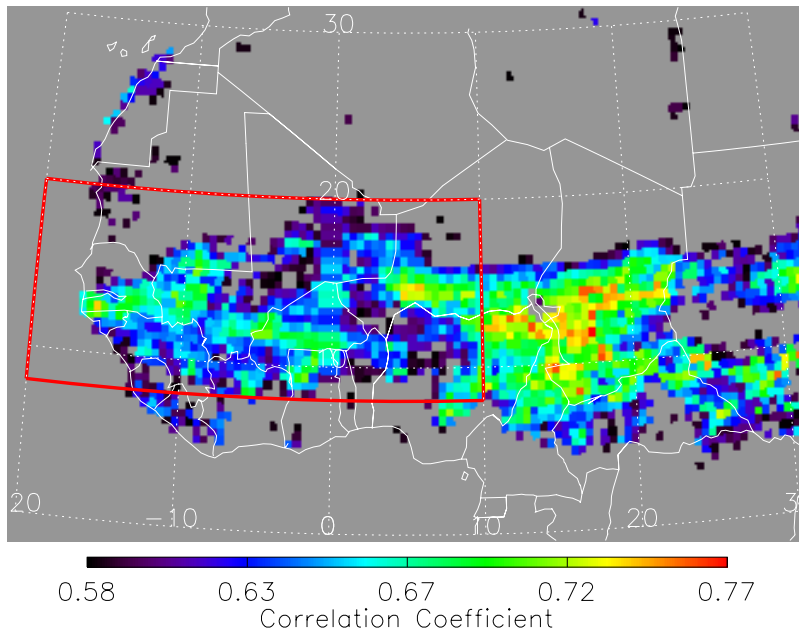
Figure 10. Correlation map of mean JFM NDVI to mean JJASO Sahel rainfall index of the previous year for 1982–2003. All values presented are statistically significant at the 99% level. The over-land area contained within the red box denotes the region used to create the mean Sahel NDVI time series.

covary on an interannual timescale while showing similar upward trends over the last 24 years.

[35] This correlation map of the JFM dust and Sahel NDVI (Figure 11) shows widespread and strong negative correlations south of 15°N, the main area of which completely fills the TATL region and extends into the southern portion of the STATL region. These correlations have a similar spatial pattern to the mean dust values from Figure 3 and fully encompass the area of negative correlations with the Sahel rainfall index from Figure 9. The mean regional correlation coefficients and significance levels from Table 2 show that on average the STATL, TATL and the TOTAL areas all covary inversely with the Sahel NDVI time series. Because the patterns of Figure 11 are found more or less below 20°N, it appears that the influence of NDVI on dust is somewhat more constrained to areas downstream of the
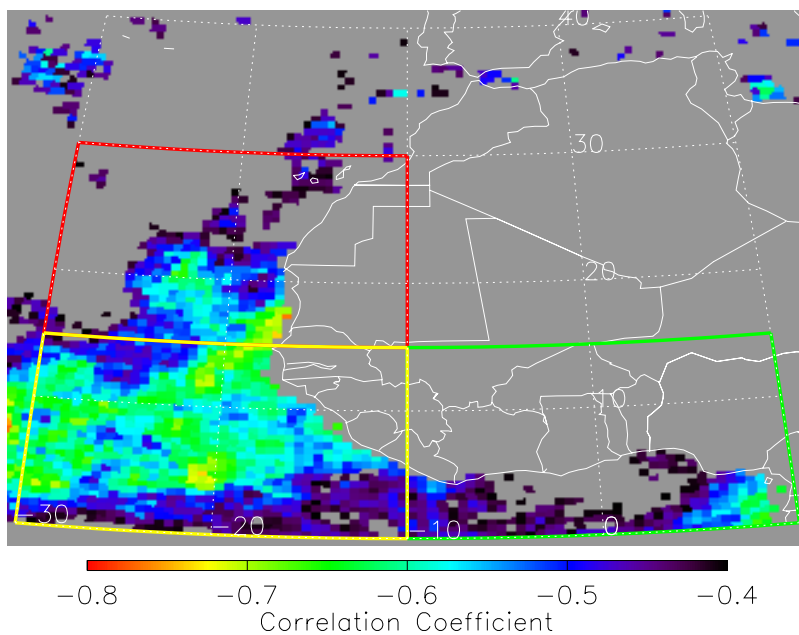

Figure 11. Correlation map of the mean JFM Sahelian NDVI to the JFM dust signal for the time period of 1982–2005. Regions of significant positive correlations were small and scattered, and therefore only negative correlations significant at the 90% level are shown. Description of boxed regions is the same as for Figure 3.

Sahel. Also, the lack of strong correlations over the Gulf of Guinea suggests that the observed Harmattan haze acts independent of influences from Sahelian vegetation.

[36] Considering the average path of the trades through the region, dust mobilization may be mediated by vegetation through increases in soil stability and reductions of wind stress on the surface, when more vegetation is present [*Gillette*, 1999]. We could infer that vegetation changes in the Sahel play an important role in dust variability. This would be consistent with the modeling studies of *Gillette* [1999] and *Engelstaedter et al.* [2003]. However, from the data presented, we cannot say absolutely that variability in dust production due to Sahel vegetation changes cause the correlation patterns from Figure 11. It is equally possible that circulation changes are causing increased summertime precipitation (resulting in Sahelian vegetation changes) and decreased wintertime dustiness concurrently.

6. Conclusions

[37] A new daytime over-water dust detection algorithm for the AVHRR has been applied to 24 years (1982–2005) of wintertime imagery over West Africa and the surrounding Atlantic utilizing a new AVHRR dust detection algorithm. The resultant time series was well correlated to similar data sets produced by the TOMS and Meteosat instruments. A climatological study showed a distinct region of enhanced mean dust values over the tropical North Atlantic and another over the Gulf of Guinea. Correlations of the dust signal with the Niño 3.4, JNAO, and Sahel rainfall indices were made. Widespread and strong correlations were found in various parts of the North Atlantic for each of the indices. Maps of these correlations were generally in agreement with previously published studies that used other satellite dust data sets to explore interannual wintertime Saharan dust variability. Furthermore, an NDVI time series responsive to variability of vegetation in the Sahel was developed and found to covary strongly with dustiness in the more tropical North Atlantic.

[38] To aid in the interpretation of the results the dust signal was divided into three regions that have been observed to show some distinct variability (Figures 3 and 4). The region over the subtropical Atlantic (STATL region, Figure 3) had the weakest dust signal, which is consistent with the seasonal cycle of dust in the region [*Husar et al.*, 1997]. We observed strong positive and negative correlations with the JNAO index and NDVI time series respectively. Also studied was an area in the more tropical Atlantic (TATL region, Figure 3), where large climatological dust mean values were found to extend from the West African coast to almost 30°W. This area was well correlated positively with the JNAO index and negatively with the Sahel rainfall index and NDVI time series. The last area studied was that of the Gulf of Guinea (HAR region, Figure 3), representative of dust entrained in the Harmattan. Here strong correlations were observed between dustiness and the Niño 3.4 and JNAO indices.

[39] With regard to the total dust signal, the NDVI time series and the JNAO index appear to be the most important factors. The difference between the two is that the JNAO was related to dustiness across the entire area studied, while the NDVI time series was more important in the TATL

region. It is possible that the JNAO is reflective of a large-scale process that exerts a degree of control on the dustiness of the areas surrounding West Africa. The correlations between the Sahel NDVI and dust coverage in the TATL region could be interpreted as signifying that vegetation in the Sahel exerts a certain amount of control on the dust in the downwind areas, considering the predominant trade flow. However, it is possible that these correlations result from general circulation features that alter summertime Sahel precipitation as well as dustiness independent of vegetation influences.

[40] This study investigated several possible influences on dust loadings around West Africa and attempted to explain the causes of the observed correlations. However, the mechanisms by which those influences play out are not always clear. This is especially true of the relationship between summertime precipitation and Sahel vegetation, as they relate to wintertime oceanic dust loadings. The increased number of channels on the more recent operational polar orbiting satellites (MODIS) can help to clarify dust source regions and how they are tied to dust aerosols observed over the North Atlantic. Also, future modeling studies with improved surface characterization will likely be important in clarifying the causes of the interannual variability of West African dust.

References

Ackerman, S. (1997), Remote sensing aerosols using satellite infrared observations, *J. Geophys. Res.*, *102*(D14), 17,069–17,079.

Alpert, P., Y. Kaufman, Y. Shay-El, D. Tanré, A. da Silvas, S. Schubert, and J. Joseph (1998), Quantification of dust-forced heating of the lower troposphere, *Nature*, *395*, 367–370.

Boyd, P., et al. (2000), A mesoscale phytoplankton bloom in the polar Southern Ocean stimulated by iron fertilization, *Nature*, *407*, 695–702.

Brooks, N., and M. Legrand (2000), Dust variability over northern Africa and rainfall in the Sahel, in *Linking Climate Change to Land Surface Change*, edited by S. J. McLaren and D. R. Kniveton, pp. 1–25, Springer, New York.

Cakmur, R. V., R. L. Miller, and I. Tegen (2001), A comparison of seasonal and interannual variability of soil dust aerosols over the Atlantic Ocean as inferred by the TOMS AI and AVHRR AOT retrievals, *J. Geophys. Res.*, *106*(D16), 18,287–18,304.

Carlson, T. N., and J. M. Prospero (1972), The large-scale movement of Saharan air outbreaks over the northern equatorial Atlantic, *J. Appl. Meteorol.*, *11*, 283–297.

Chiapello, I., and C. Moulin (2002), TOMS and Meteosat satellite records of the variability of Saharan dust transport over the Atlantic during the last two decades (1979–1997), *Geophys. Res. Lett.*, *29*(8), 1176, doi:10.1029/2001GL013767.

Chiapello, I., C. Moulin, and J. Prospero (2005), Understanding the long-term variability of African dust transport across the Atlantic as recorded in both Barbados surface concentrations and large-scale Total Ozone Mapping Spectrometer (TOMS) optical thickness, *J. Geophys. Res.*, *110*, D18S10, doi:10.1029/2004JD005132.

Dunion, J. P., and C. S. Velden (2004), The impact of the Saharan air layer on Atlantic tropical cyclone activity, *Bull. Am. Meteorol. Soc.*, *90*, 353–365.

Engelstaedter, S., K. Kohfeld, I. Tegen, and S. Harrison (2003), Controls of dust emissions by vegetation and topographic depressions: An evaluation using dust storm frequency data, *Geophys. Res. Lett.*, *30*(6), 1294, doi:10.1029/2002GL016471.

Evan, A. T., A. K. Heidinger, and M. J. Pavolonis (2006), Development of a new over–water advanced very high resolution radiometer dust detection algorithm, *Int. J. Remote Sens.*, in press.

Foley, J. A., M. T. Coe, M. Scheffer, and G. Wang (2003), Regime shifts in the Sahara and Sahel: Interactions between ecological and climatic systems in northern Africa, *Ecosystems*, *6*, 524–539, doi:10.1007/s10021-002-0227-0.

Gillette, D. (1999), A qualitative geophysical explanation for "hot spot" dust emitting source regions, *Contrib. Atmos. Phys.*, *72*, 67–77.

Ginoux, P., J. M. Prospero, O. Torres, and M. Chin (2004), Long-term simulation of global dust distribution with the GOCART model: Correlation with North Atlantic Oscillation, *Environ. Modell. Software*, *19*, 113–128.

Goudie, A. S., and N. J. Middleton (2001), Saharan dust storms: Nature and consequences, *Earth Sci. Rev.*, *56*, 179–204.

Hastenrath, S. (1991), *Climate Dynamics of the Tropics*, 488 pp., Springer, New York.

Heidinger, A., V. Anne, and C. Dean (2001), Using MODIS to quantify cloud contamination in the AVHRR data-record, *J. Atmos. Oceanic Technol.*, *19*, 586–601.

Heidinger, A., C. Cao, and J. T. Sullivan (2002), Using Moderate Resolution Imaging Spectrometer (MODIS) to calibrate advanced very high resolution radiometer reflectance channels, *J. Geophys. Res.*, *107*(D23), 4702, doi:10.1029/2001JD002035.

Hurrell, J. (1995), Decadal trends in the North Atlantic Oscillation and relationships to regional temperature and precipitation, *Science*, *269*, 676–679.

Husar, R., J. Prospero, and L. Store (1997), Characterization of tropospheric aerosols over the oceans with the NOAA advanced very high resolution radiometer optical thickness operational product, *J. Geophys. Res.*, *102*(D14), 16,889–16,909.

Janowiak, J. (1988), An investigation of interannual rainfall variability in Africa, *J. Clim.*, *1*, 240–255.

Jankowiak, I., and D. Tanré (1992), Satellite climatology of Saharan dust outbreaks: Method and preliminary results, *J. Clim.*, *5*, 646–656.

Jones, P., T. Jünsson, and D. Wheeler (1997), Extensions to the North Atlantic Oscillation using early instrumental pressure observations from Gibraltar and south-west Iceland, *Int. J. Climatol.*, *17*, 1433–1450.

Kalnay, E., et al. (1996), The NCEP/NCAR reanalysis 40–year project, *Bull. Am. Meteorol. Soc.*, *77*, 437–471.

Kaufman, Y. J., I. Koren, L. Remer, D. Tanré, P. Ginoux, and S. Fan (2003), Dust transport and deposition observed from the Terra-MODIS spacecraft over the Atlantic Ocean, *Bull. Am. Meteorol. Soc.*, *90*, 1–12.

Knippertz, P., and A. H. Fink (2006), Synoptic and dynamic aspects of an extreme springtime Saharan dust outbreak, *Q. J. R. Meteorol. Soc.*, in press.

Mahowald, N. M., and L. M. Kiehl (2003), Mineral aerosol and cloud interactions, *Geophys. Res. Lett.*, *30*(9), 1475, doi:10.1029/2002GL016762.

Mahowald, N., C. Luo, J. del Corral, and C. S. Zender (2003), Interannual variability in atmospheric mineral aerosols from a 22-year model simulation and observational data, *J. Geophys. Res.*, *108*(D12), 4352, doi:10.1029/2002JD002821.

Martin, J. H. (1994), Testing the iron hypothesis in ecosystems of the equatorial Pacific Ocean, *Nature*, *371*, 123–129.

McClain, E. P. (1989), Global sea surface temperatures and cloud clearing for aerosol optical depth estimates, *Int. J. Remote Sens.*, *10*, 763–769.

McClain, E. P., W. G. Pichel, and C. C. Walton (1985), Comparative performance of AVHRR-based multichannel sea surface temperatures, *J. Geophys. Res.*, *90*(C6), 11,587–11,601.

Middleton, N. J., and A. S. Goudie (2001), Saharan dust: Sources and trajectories, *Trans. Inst. Br. Geogr.*, *26*, 165–181.

Miller, R., and I. Tegen (1998), Climate response to soil dust aerosols, *J. Clim.*, *11*, 3247–3267.

Moulin, C., and I. Chiapello (2004), Evidence of the control of summer atmospheric transport of African dust over the Atlantic by Sahel sources from TOMS satellites (1979–2000), *Geophys. Res. Lett.*, *31*, L02107, doi:10.1029/2003GL018931.

Moulin, C., C. Lambert, F. Dulac, and U. Dayan (1997), Control of atmospheric export of dust from North Africa by the North Atlantic Oscillation, *Nature*, *387*, 691–694.

Nalli, N., and L. Stowe (2002), Aerosol correction for remotely sensed sea surface temperatures from the National Oceanic and Atmospheric Administration advanced very high resolution radiometer, *J. Geophys. Res.*, *107*(C10), 3172, doi:10.1029/2001JC001162.

Nicholson, S. E. (1981), Rainfall and atmospheric circulation during drought periods and wetter years in Africa, *Mon. Weather Rev.*, *109*, 2191–2208.

Nicholson, S. E., and J. Y. Kim (1997), The relationship of the El Niño–Southern Oscillation to African rainfall, *Int. J. Climatol.*, *17*, 117–135.

Prospero, J. M. (1999), Assessing the impact of advected African dust on air quality and health in the eastern United States, *Human Ecol. Risk Assess.*, *5*, 471–479.

Prospero, J. M., and P. Lamb (2003), African droughts and dust transport to the Caribbean: Climate change implications, *Science*, *302*, 1024–1027.

Prospero, J. M., and R. Nees (1977), Dust concentration in the atmosphere of the equatorial North Atlantic: Possible relationship to the Sahelian drought, *Science*, *196*, 1196–1198.

Prospero, J. M., and R. Nees (1986), Impact of the North African drought and El Niño on mineral dust in the Barbados trade winds, *Nature*, *320*, 735–738.

Prospero, J. M., P. Ginoux, O. Torres, S. Nicholson, and T. Gill (2002), Environmental characterization of global sources of atmospheric soil dust identified with the Nimbus 7 Total Ozone Mapping Spectrometer (TOMS) absorbing aerosol product, *Rev. Geophys.*, *40*(1), 1002, doi:10.1029/2000RG000095.

Sassen, K., P. DeMott, J. Prospero, and M. Poellot (2003), Saharan dust storms and indirect aerosol effects on clouds: CRYSTAL-FACE results, *Geophys. Res. Lett.*, *30*(12), 1633, doi:10.1029/2003GL017371.

Shinn, E., G. Smith, J. Prospero, P. Betzer, M. Hayes, V. Garrison, and R. Barber (2000), African dust and the demise of Caribbean coral reefs, *Geophys. Res. Lett.*, *27*(19), 3029–3032.

Sokolik, I., D. Winker, G. Bergametti, D. Gillette, G. Carmichael, Y. Kaufman, L. Gomes, L. Schultz, and J. Penner (2001), Introduction to special section: Outstanding problems in quantifying the radiative impacts of mineral dust, *J. Geophys. Res.*, *106*(D16), 18,015–18,027.

Stallard, R. (2001), Possible environmental factors underlying amphibian decline in eastern Puerto Rico: Analysis of U.S. government data archives, *Conserv. Biol.*, *15*, 943–955.

Swap, R., M. Garstang, S. Greco, R. Talbot, and P. Kallberg (1992), Saharan dust in the Amazon Basin, *Tellus, Ser. B*, *44*, 133–149.

Swap, R., S. Ulanski, M. Cobbett, and M. Garstang (1996), Temporal and spatial characteristics of Saharan dust outbreaks, *J. Geophys. Res.*, *101*(D2), 4205–4220.

Thomas, S., and K. Heidinger (2004), Comparison of NOAA's operational AVHRR derived cloud amount to other satellite derived cloud climatologies, *J. Clim.*, *17*(24), 4805–4822.

Ward, M. N. (1998), Diagnosis and short-lead time prediction of summer rainfall in tropical North Africa at interannual and multidecadal timescales, *J. Clim.*, *11*(12), 3167–3191.

Washington, R., and M. C. Todd (2005), Atmospheric controls on mineral dust emission from the Bodélé Depression, Chad: The role of the low level jet, *Geophys. Res. Lett.*, *32*, L17701, doi:10.1029/2005GL023597.

Zender, C. S., and E. Y. Kwon (2005), Regional contrasts in dust emission responses to climate, *J. Geophys. Res.*, *110*, D13201, doi:10.1029/2004JD005501.

————————————
A. T. Evan, Cooperative Institute for Meteorological Satellite Studies, University of Wisconsin–Madison, 1225 West Dayton Street, Madison, WI 53706, USA. (atevan@wisc.edu)

A. K. Heidinger, Office of Research and Applications, NESDIS, NOAA, 1225 West Dayton Street, Madison, WI 53706, USA.

P. Knippertz, Institute of Atmospheric Physics, University of Mainz, D-55099 Mainz 1225, Germany.